The Photosynthetic Reaction Center from the Purple Bacterium *Rhodopseudomonas viridis*

JOHANN DEISENHOFER AND HARTMUT MICHEL

The history and methods of membrane protein crystallization are described. The solution of the structure of the photosynthetic reaction center from the bacterium *Rhodopseudomonas viridis* is described, and the structure of this membrane protein complex is correlated with its function as a light-driven electron pump across the photosynthetic membrane. Conclusions about the structure of the photosystem II reaction center from plants are drawn, and aspects of membrane protein structure are discussed.

AS IN MANY INSTANCES OF NEW SCIENTIFIC DEVELOPMENTS and technical inventions, an accidental observation caused the beginning of the experiments that resulted in the elucidation of the three-dimensional structure of a photosynthetic reaction center. This initiating observation, made in 1978, was of solid, most likely glass-like aggregates that formed when bacteriorhodopsin, delipidated according to Happe and Overath (*1*), was stored in the freezer (Fig. 1A). I (H.M.) was convinced that it should be possible not only to obtain these solid bodies, but also to produce three-dimensional crystals.

The availability of well-ordered three-dimensional crystals is the prerequisite for a high-resolution x-ray crystallographic analysis of large biological macromolecules. However, at that time the crystallization of membrane proteins was considered to be impossible. I was working at the University of Wüerzburg as a postdoc in D. Oesterhelt's lab, who with W. Stockenius discovered bacteriorhodopsin (*2*) and proposed its function (*3*). Bacteriorhodopsin, the protein component of the "purple membrane" acts as a light-energy converting system in halobacteria. It is an integral membrane protein that forms two-dimensional crystals in the purple membrane.

The Crystallization

After several failures, which, however, lead to the formation of a new two-dimensional crystal form of bacteriorhodopsin, a new strategy was developed based on the properties of membrane proteins (*4*). Membrane proteins are embedded into the electrically insulating lipid bilayers. Membrane proteins are difficult to handle because they have a hydrophobic surface in contact with the alkane chains of the lipids and a polar surface in contact with the aqueous phases on both sides of the membrane and the polar head groups of the lipids (Fig. 2A). As a result, membrane proteins are not soluble in aqueous buffers or in organic solvents of low dielectric constant, and therefore one has to add detergents. The detergent micelles take up the membrane proteins and shield the hydrophobic surface parts of the membrane protein from contact with water (Fig. 2B). The membrane protein in the detergent micelle then has to be purified by the various chromatographic procedures. Once the protein has been isolated and is available in large quantities, one can try to crystallize it. For membrane proteins that are merely anchored in the membrane, the most promising approach is to remove the membrane anchor by proteases or to use genetically modified material where the part of the gene coding for the membrane anchor has been deleted. For truly integral membrane proteins, two possibilities exist to form crystals: (i) stacks of two-dimensional crystals (Fig. 2C, type I), and (ii) membrane proteins crystallized within the detergent micelles (Fig. 2D, type II). The type II crystal appears to be easier to achieve; the crystal lattice will be formed by the membrane proteins via polar interactions between polar surface parts. Membrane proteins with large extramembranous domains should form type II crystals much more easily than those with small polar domains. The size of the detergent micelle is crucial. A large detergent micelle might prevent the required close contact between the polar surface domains of the membrane proteins. One way to achieve a small detergent micelle is to use small linear detergents like octylglucopyranoside. However, membrane proteins in micelles formed by a detergent with a short alkyl chain are usually not very stable. An increase of the alkyl chain length by one methylene group frequently leads to an increase of the stability by a factor of 2 to 3. One therefore has to find a compromise.

The advantage of the type II crystals is that basically the same procedures to induce supersaturation of the membrane protein solution can be used as for soluble proteins, namely vapor diffusion or dialysis with salts or polymers such as polyethylene glycol as precipitating agents. However, a viscous detergent phase often forms, which seems to consist of precipitated detergent micelles (*5*). Membrane proteins are enriched in the detergent phase and frequently undergo denaturation. In several examples, crystals that were already formed are redissolved.

The improvement. The lack of success with bacteriorhodopsin was always that the detergent micelles still were too large. The use of even smaller detergents was impossible because of the insufficient stability of bacteriorhodopsin in detergents with a shorter alkyl

J. Deisenhofer is at Howard Hughes Medical Institute and Department of Biochemistry, University of Texas Southwestern Medical Center at Dallas, 5323 Harry Hines Blvd., Dallas, TX 75235-9050. H. Michel is at Max-Planck-Institute for Biophysics, Heinrich-Hoffmann-Strasse 7, D-6000 Frankfurt/M 71, Federal Republic of Germany.
This article is a combined version of the lectures the authors delivered in Stockholm, Sweden, 8 December 1988, when they received the Nobel Prize for Chemistry, which they shared with Robert Huber. It is published here with the permission of the Nobel Foundation.

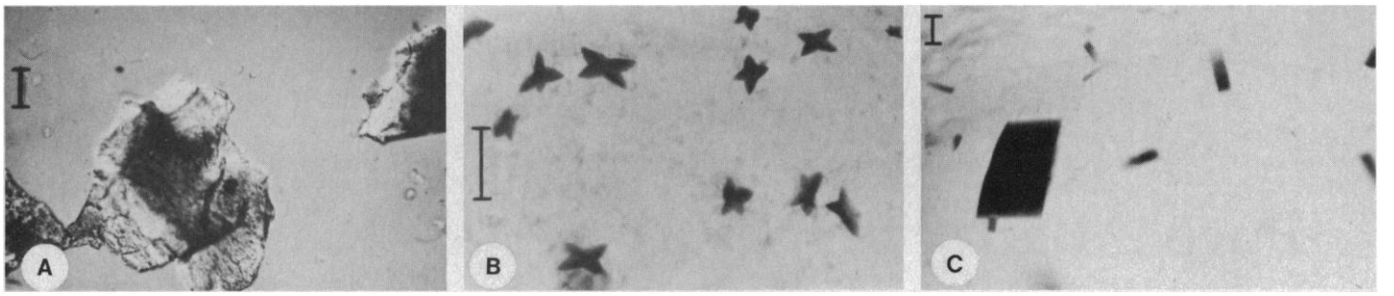

Fig. 1. Optical micrograph showing crystals and aggregates of bacteriorhodopsin and the photosynthetic reaction center from *Rps. viridis*. (**A**) Glass-like aggregates of bacteriorhodopsin obtained after freezing of delipidated bacteriorhodopsin. (**B**) Star-like reaction center crystals obtained within 2 days (starting conditions: 1 mg of protein per milliliter, 3% heptane-1,2,3-triol, and 1.5*M* ammonium sulfate) by vapor diffusion against 3*M* ammonium sulfate (*8*). (**C**) Tetragonal crystals of the reaction center obtained within 3 weeks [starting conditions as in (A)] by vapor diffusion against 2.4*M* ammonium sulfate (*8*). Bar, 0.1 mm (in all photographs).

chain or a smaller polar head group. Small amphiphilic molecules (*4, 6*) were used for several reasons. (i) These molecules might displace detergent molecules, which were too large to fit perfectly into the protein's crystal lattice in certain positions. (ii) The small amphiphilic molecules are too small to form micelles themselves, but they are incorporated into the detergent micelles. These mixed micelles are smaller than the pure detergent micelles and possess a different curvature of their surface; as a result the proteins could come closer together. (iii) The polar head group of small amphiphilic molecules is smaller than that of the detergent, and less of the protein's polar surface would be covered by the polar part of the mixed small amphiphile–detergent micelle.

The turn to classical photosynthesis. Frustrated from the lack of the final breakthrough with bacteriorhodopsin, which is partly caused by the absence of large extramembranous domains in this protein, the purple bacteria *Rhodospirillum rubrum* and *Rhodopseudomonas viridis* and the light-harvesting chlorophyll a/b protein from spinach were pursued instead. These colored proteins (or protein complexes) were thought to be part of a two-dimensional crystalline array already in their native environment, were available in large quantities, and easily isolated. Denaturation was indicated by color changes. When the reaction centers from *Rps. viridis* were isolated by using hydroxyapatite chromatography according to a published procedure (*7*), the crystallization attempts were without success. When the reaction centers were isolated by using only molecular sieve chromatography, crystals were obtained immediately (*8*). The conditions were nearly identical to those found to be optimal for bacteriorhodopsin. The exception was that we could use *N,N*-dimethyldodecylamine *N*-oxide as detergent instead of octylglucopyranoside. In the presence of 3% heptane-1,2,3-triol (a high melting point isomer) and 1.5 to 1.8*M* ammonium sulfate, star-like crystals are obtained upon vapor diffusion against 2.5 to 3*M* ammonium sulfate in 2 days, and more regular tetragonal columns were obtained with a length of up to 2 mm on vapor diffusion against 2.2 to 2.4*M* ammonium sulfate in 2 to 3 weeks (Fig. 1, B and C). The much smaller polar head group of *N,N*-dimethyldodecylamine *N*-oxide is certainly of importance, but unfortunately this detergent denatures bacteriorhodopsin. D. Oesterhelt generously considered the reaction center as my project. The crystals turned out to be of excellent quality from the beginning, and diffracted to a resolution of 2.5 Å (*8*).

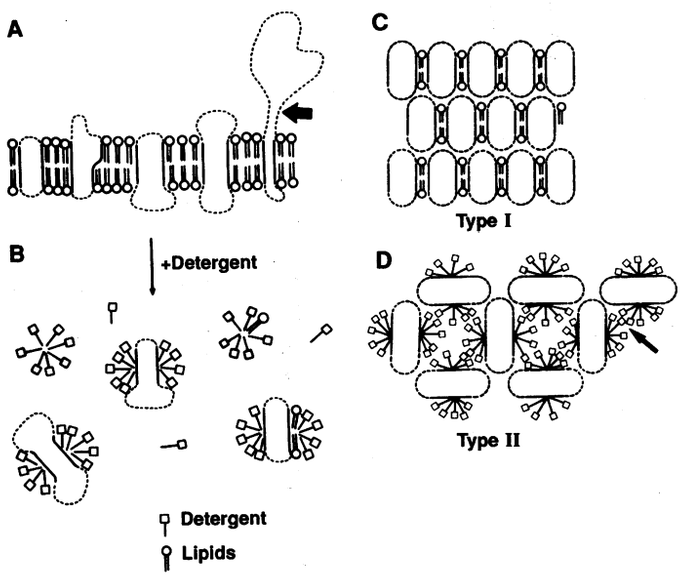

Fig. 2. (**A**) Schematic drawing of a biological membrane consisting of a lipid bilayer and membrane proteins embedded into it and (**B**) its solubilization by detergents. The polar part of the membrane protein surface is indicated by broken lines (*11*). (C and D) The two basic types of membrane protein crystals. (**C**) Type I: stacks of membranes containing two-dimensional crystalline membrane proteins, which are then ordered in the third dimension. (**D**) Type II: a membrane protein crystallized with detergents bound to its hydrophobic surface. The polar surface part of the membrane proteins is indicated by broken lines.

Structure Determination

In spring 1982 I (J.D.) joined H.M. in order to determine the three-dimensional structure of the reaction center. The tetragonal crystals have unit cell dimensions of $a = b = 223.5$ Å, $c = 113.6$ Å, and the symmetry of space group $P4_32_12$ (*8, 9*). As it turned out, there is one reaction center with a molecular size of 145,000 daltons in the asymmetric unit. To solve the phase problem for the reaction center crystal structure, we used the method of isomorphous replacement with heavy atom compounds. A number of heavy atom compounds could not be used since they induced the phase separation of the soak buffer into the viscous detergent phase and the aqueous phase. Additional purification of the reaction centers before crystallization was necessary to obtain crystals of useful heavy atom derivatives with undisturbed diffraction quality. Using five different heavy atom derivatives with an average of nine heavy atom binding sites each, we could calculate phases to 3.0 Å resolution and an electron density map (*9*), which were further improved by solvent flattening (*10*).

Map interpretation and model building was done in three stages. At first the prosthetic groups in the reaction center were identified (*9*). Next, the polypeptide chains were built with polyalanine sequence, except in the NH_2-terminal regions of the subunits L, M, and cytochrome where partial amino acid sequences were known

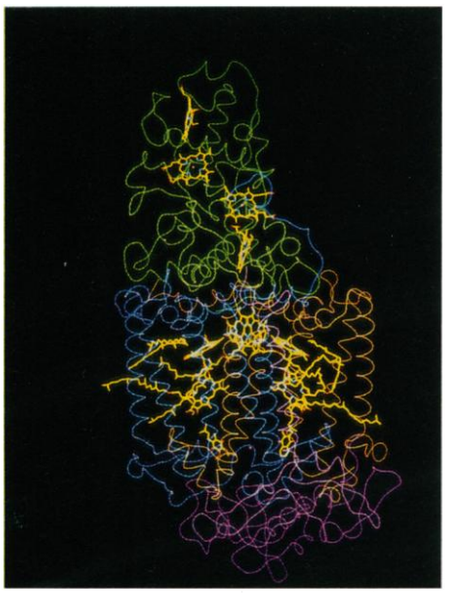

Fig. 3. Overall view of the reaction center structure. Protein chains are represented as smoothed backbone drawings; green, cytochrome; blue, M subunit; brown, L subunit; purple, H subunit. Cofactors are represented in bright atom colors as follows: yellow, carbons; blue, nitrogens; red, oxygens; and green, magnesium.

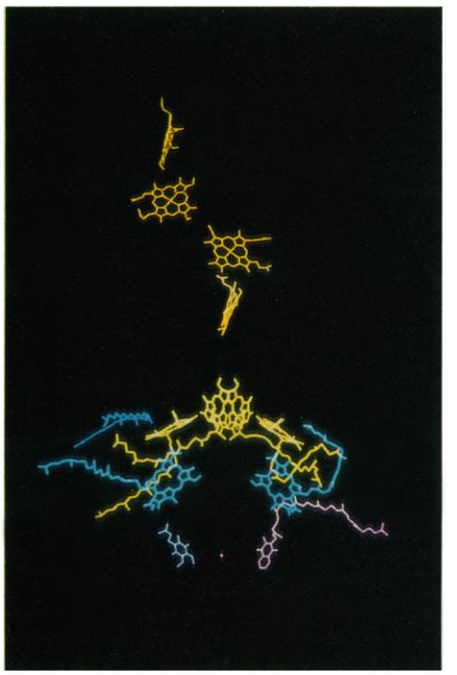

Fig. 5. The cofactors. Dark yellow, heme groups; yellow, BC-b's; light blue, bacteriopheophytin-b's; blue, carotenoid [dihydro-neurosporene (*66*)]; purple, quinones (right, Q_A; left, Q_B); and purple dot, nonheme iron.

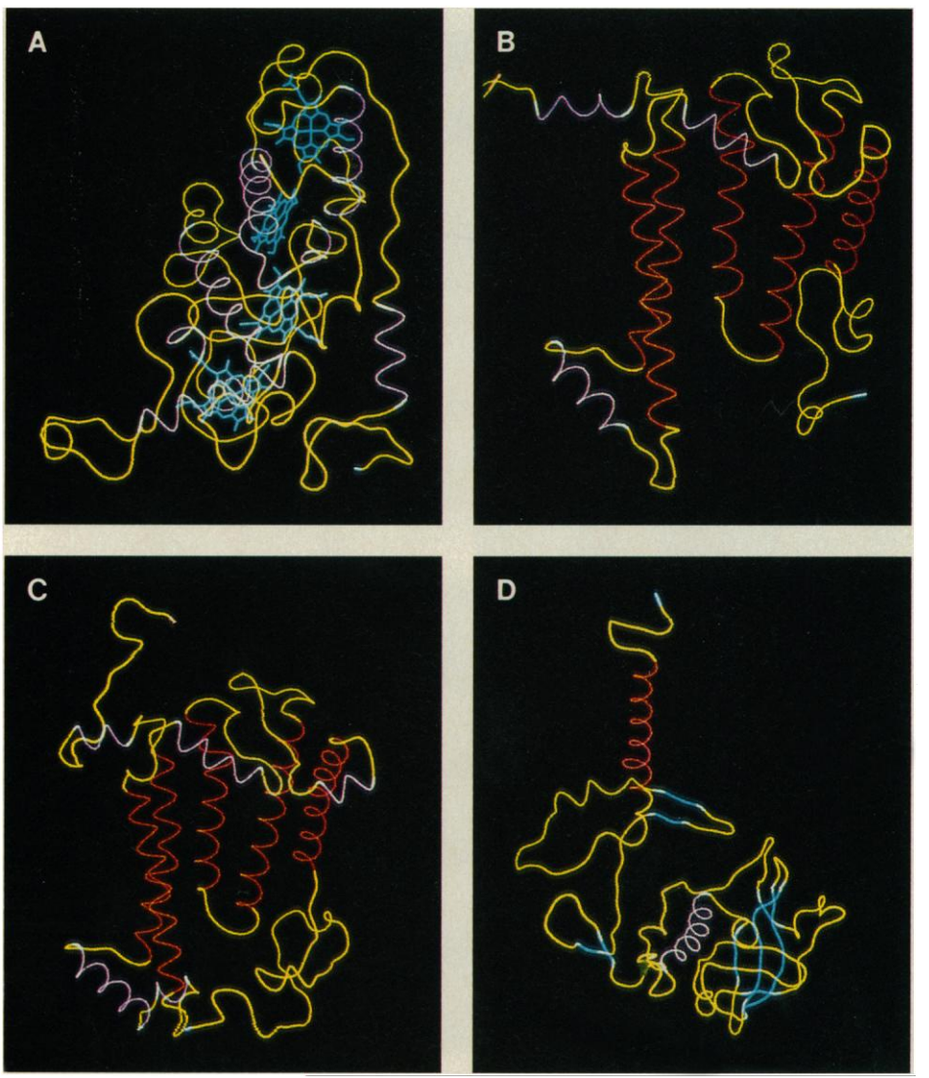

Fig. 4. Smoothed backbone representations of the protein subunits. Secondary structure is indicated by colors. Yellow, no apparent secondary structure; red, transmembrane helices; purple, other helices; blue, antiparallel β sheets. (**A**) Cytochrome (with the four heme groups); (**B**) L subunit; (**C**) M subunit; and (**D**) H subunit. Amino termini are marked blue and COOH-termini are marked red.

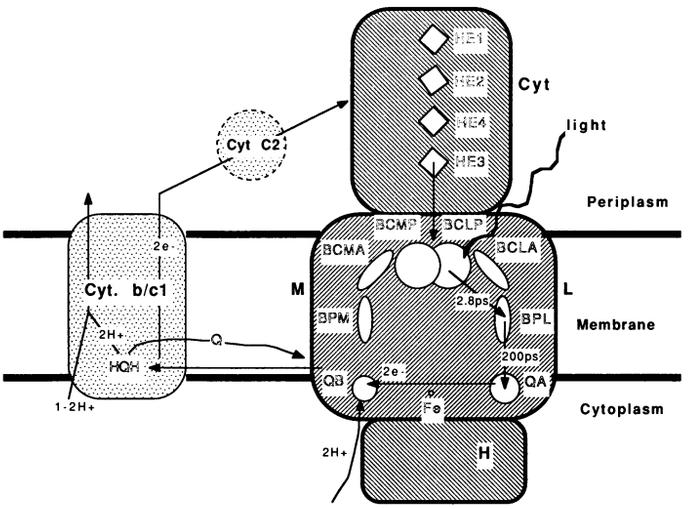

Fig. 6. Schematic view of the reaction center showing the light-driven cyclic electron flow.

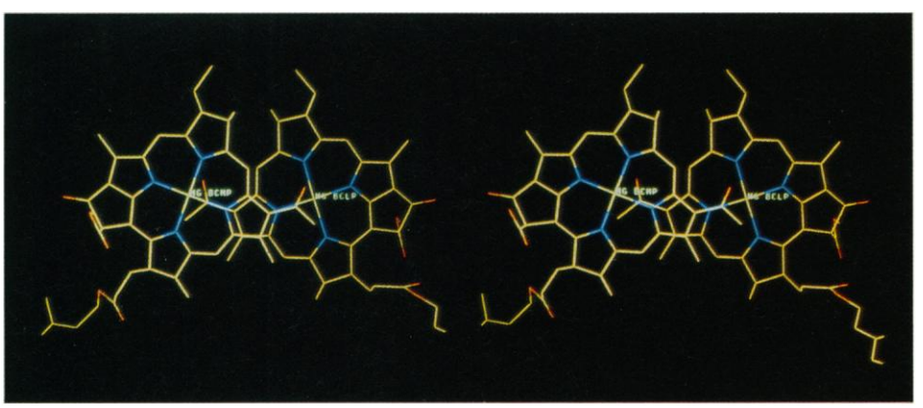

Fig. 7. Stereo view of P in atom colors: yellow, carbons; blue, nitrogens; red, oxygens; and green, magnesium.

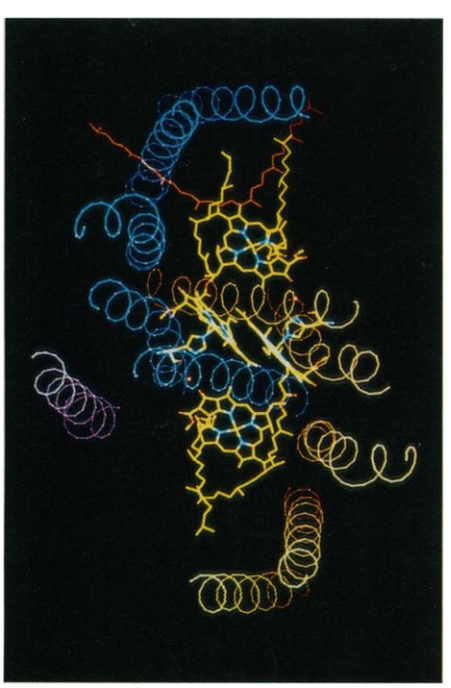

Fig. 8. View along the central local twofold axis showing in atom colors: P with His ligands, accessory BC-b's (BC_{LA} bottom, BC_{MA} top), and two water molecules; the transmembrane helices of subunits L (brown), M (blue), and H (purple) are shown in smoothed backbone representation.

(*11*) and could be used to distinguish between the subunits (*12*). Finally, as the gene sequences of the reaction center subunits were determined (*13–15*), the model of the protein subunits was completed.

The reaction center model, with about half of the side chains of the cytochrome subunit still missing, already had the rather low crystallographic R value of 0.359 at 2.9 Å resolution (*12*) [$R = \Sigma(||F_{obs}| - |F_{calc}||)/\Sigma|F_{obs}|$; F_{obs} and F_{calc} are observed and calculated structure factors, respectively]. Crystallographic refinement of the model was started at 2.9 Å resolution and continued at 2.3 Å resolution. The program packages used for refinement were PROTEIN, EREF (*16, 17*), TNT (*18*), and FRODO (*19*).

As a result of the refinement, the R value was brought down to 0.193 for 95762 unique reflections at 2.3 Å resolution; the refined model consists of 10288 nonhydrogen atoms. Errors in the initial model (for example, peptide groups and side chains with wrong orientations) were removed. New features were added to the model: a partially ordered carotenoid molecule, a ubiquinone in the partially occupied Q_B binding pocket, a complete detergent molecule (LDAO), a candidate for a partially ordered LDAO or similar molecule, seven candidates for negative ions, and 201 ordered water molecules. The upper limit of the mean coordinate error was estimated (*20*) to be 0.26 Å. A detailed description of refinement and refined model of the photosynthetic reaction center from *Rps. viridis* will be given elsewhere (*21*).

Structure and Function

Structure overview. The photosynthetic reaction center from *Rps. viridis* is a complex of four protein subunits [H (heavy), M (medium), L (light), and cytochrome] and 14 cofactors (Fig. 3). The total length of the reaction center, from the tip of the cytochrome to the H subunit is about 130 Å. The core has an elliptical cross section with axes of 70 and 30 Å. The core of the complex is formed by subunits L and M and their associated cofactors: four bacteriochlorophyll-b's (BC-b), two bacteriopheophytin-b's (BP-b), one nonheme iron, two quinones, and one carotenoid. Structural properties and functional considerations indicate that subunits L and M span the bacterial membrane. Each of the subunits L and M contains five membrane-spanning polypeptide segments, folded into long helices. The polypeptide segments connecting the transmembrane helices form flat surfaces parallel to the membrane surfaces.

The H subunit contributes another membrane-spanning helix with its NH_2 terminus near the periplasmic membrane surface. The COOH-terminal half of the H subunit forms a globular domain that is bound to the L-M complex near the cytoplasmic membrane surface. On the opposite side of the membrane, the cytochrome subunit with its four covalently bound heme groups is attached to the L-M complex. Both the cytochrome subunit and the globular domain of the H subunit have surface properties typical for water-soluble proteins.

Subunit structure. The polypeptide chain folding of the four reaction center subunits are shown in Fig. 4. Structurally similar segments in the L and M subunits include the transmembrane helices and a large fraction of the connections. In total, 216 α carbons from the M subunit (323 residues) can be superimposed onto corresponding α carbons of the L subunit (273 residues) with

a root mean square (rms) deviation of only 1.22 Å. The superposition of the subunits is done by a rotation of about 180° around an axis running perpendicular to the membrane surface; we call this axis the central local symmetry axis (Tables 1 and 2). In addition to the transmembrane helices, with lengths between 21 and 28 residues, there are shorter helices in the connecting segments. Insertions at the NH_2- and COOH-termini make the M subunit dominate the contacts with the peripheral subunits. The insertion between transmembrane helices MD and ME, containing another small helix (Table 1), is of importance for the different conformations of the quinone binding sites in L and M and for binding of the nonheme iron.

The H subunit with 258 residues can be divided into three structural regions with different characteristics (Fig. 4). The NH_2-terminal segment, beginning with formyl-methionine (*13*), contains the only transmembrane helix of subunit H; it includes 24 residues from H12 to H35. Near the end of the transmembrane helix, the sequence shows seven consecutive charged residues (H33 to H39). Residues H47 to H53 are disordered in the crystal, and therefore no significant electron density can be found for them.

Following the disordered region, the H chain forms an extended structure along the surface of the L-M complex, apparently deriving structural stability from that contact. The surface region contains a short helix and two two-stranded antiparallel β sheets.

The third structural segment of the H subunit, starting at about H105, forms a globular domain. This domain contains an extended system of antiparallel and parallel β sheets between residues H134 and H203 and an α helix (residues H232 to H248). The β-sheet region, the only larger one in the whole reaction center, forms a pocket with highly hydrophobic interior walls. So far, no evidence for a ligand has been found.

With 336 residues (*15*), the cytochrome is the largest subunit in the reaction center complex. Its last four residues, C333 to C336, are disordered. Also disordered is the lipid moiety bound to the NH_2-terminal Cys residue (*22*). The complicated structure of the cytochrome can be summarized as follows: the structure consists of an NH_2-terminal segment, two pairs of heme-binding segments, and a segment connecting the two pairs. Each heme-binding segment consists of a helix with an average length of 17 residues, followed by a turn and the Cys-X-Y-Cys-His sequence typical for c-type cytochromes. The hemes are connected to the Cys residues via thioether linkages. This arrangement leads to the heme planes being parallel to the helix axes. The sixth ligands to the heme irons are, in three of the four cases, Met residues within the helices. The iron of heme 4 has His C124, located in a different part of the structure, as a sixth ligand. The two pairs of heme-binding segments, containing hemes 1 and 2, and 3 and 4, respectively, are related by a local twofold symmetry. From each pair, 65 residues obey this local symmetry with an rms deviation between corresponding α carbon atoms of 0.93 Å. The local symmetry of the cytochrome is not related to the central local symmetry.

Table 1. Helical segments in subunits L and M (length is number of residues).

Helix	Segment (length)	
	Subunit L	Subunit M
	Transmembrane	
A	L33–L53 (21)	M52–M76 (25)
B	L84–L111 (28)	M111–M137 (27)
C	L116–L139 (24)	M143–M166 (24)
D	L171–L198 (28)	M198–M223 (26)
E	L226–L249 (24)	M260–M284 (25)
	Periplasmic	
		M81–M87 (7)
cd	L152–L162 (11)	M179–M190 (12)
ect	L259–L267 (9)	M292–M298 (7)
	Cytoplasmic	
		M232–M237 (6)
de	L209–L220 (12)	M241–M254 (14)

Table 2. Regions with similar polypeptide-chain folding in subunits L and M (length is number of residues).

Subunit M	Subunit L	Length
M49–M76 →	L29–L56	28
M88–M96 →	L61–L69	9
M100–M224 →	L73–L197	125
M243–M290 →	L209–L256	48
M291–M296 →	L258–L263	6

Arrangement of cofactors. The arrangement of the 14 cofactors associated with the reaction center protein subunits is shown in Fig. 5. The four heme groups of the cytochrome, numbered according to the order of attachment to the protein, form a linear chain that points to a closely associated pair of BC-b's. This pair, the "special pair" (P) is the origin of two branches of cofactors, each consisting of another BC-b (the "accessory" BC-b), a BP-b, and a quinone. The nonheme iron sits between the quinones. The tetrapyrrole rings of BC-b's, BP-b's, and quinones approximately follow the same local symmetry that is displayed by the L and M chains. The branches of cofactors from P to the BP-b's can be clearly associated with subunits L or M, so that they can be referred to as an L branch and an M branch. The basis for our nomenclature is as follows: BC-b and BP-b are called BC_{XY} and BP_X, respectively, where X denotes the branch (L or M) and Y is P or A for "accessory." At the level of the quinones, the situation is more complicated because the subunits interpenetrate here, and the quinone at the end of the L branch is actually bound in a pocket of the M subunit and vice versa. Therefore, we prefer the nomenclature Q_A and Q_B with Q_A at the end of the L branch; Q_A is menaquinone-9 and Q_B is ubiquinone-9 (*23*). The local symmetry is violated by the phytyl chains of BC-b's and BP-b's, by the different chemical nature and different occupancy of the quinones, and by the presence of a carotenoid molecule near the accessory BC-b of the M branch.

Functional overview. The current understanding of the function of the reaction center was developed by combining structural information with information from other experimental techniques, notably spectroscopy (for reviews see *24–26*). A schematic view of the reaction center with its cofactors in the bacterial membrane is shown in Fig. 6. P is the starting point for a light-driven electron transfer reaction across the membrane. Absorption of a photon, or energy transfer from light-harvesting complexes in the membrane, puts P into an excited state (P*). From P* an electron is transferred to the BP-b on the L branch, BP_L, with a time constant of 2.8 ps (*27, 28*). The distinction between the two BP-b's was possible because they absorb at slightly different wavelengths, and, with the knowledge of the crystal structure, linear dichroism absorption experiments could distinguish between the two chromophores (*29–31*).

From BP_L the electron is transferred to Q_A with a time constant of ~200 ps. At this point the electron has crossed most of the membrane. From Q_A the electron moves on to Q_B within about 100 μs. The nonheme iron does not seem essential in this step (*32*). Q_B can pick up two electrons and, subsequently, two protons (*33*). In the Q_BH_2 state Q_B dissociates from the reaction center, and the Q_B site is refilled from a pool of quinones dissolved in the membrane. Electrons and protons on Q_BH_2 are transferred back through the membrane by the cytochrome b-c_1 cytochrome complex. The electrons are shuttled via a soluble cytochrome c_2 to the reaction center's

cytochrome, from which P^+ had been reduced with a time constant of ~270 μs. The whole process can be described as a light-driven cyclic electron flow, the net effect of which is the generation of a proton gradient across the membrane that is used to synthesize adenosine triphosphate (ATP), as described by P. Mitchell's chemiosmotic theory (*34*).

Complete understanding of the reaction center's function still meets with a number of problems. The nature of electron transfer along the stages described above (its speed and temperature dependence) has not yet been explained theoretically. The first step, with the question of the role of the bridging BC_{LA}, is a matter of fascinating debate.

One of the major surprises from the structural work was the symmetry of the core structure, raising the question of the factors leading to the use of only the L branch of cofactors and of the significance of the apparently unused branch. Further questions relate to electron transfer between Q_A and Q_B, the role of the nonheme Fe, and the function of Q_B as a two-electron gate and proton acceptor. Finally, the purpose of the cytochrome, as well as details of electron transfer from the soluble cytochrome and among the four hemes has not been completely explained.

The special pair. The BC-b–ring systems of P, the primary electron donor of the photosynthetic light reaction, is shown in Fig. 7. On the basis of spin resonance experiments, the existence of P had been postulated a long time ago (*35*). The overlap of the pyrrole rings I of the molecules is such that, when looking in a direction perpendicular to the ring planes, the atoms of these rings eclipse each other. The orientation of the rings leads to a close proximity between the ring I acetyl groups and the Mg^{2+} ions; however, the acetyl groups do not act as ligands to the Mg^{2+}. The pyrrole rings I of both BC-b's are nearly parallel and ~3.2 Å apart. Both tetrapyrrole rings, however, are nonplanar; planes through the pyrrole nitrogens of each BC-b form an angle of 11.3°.

Local symmetry. The P BC-b's are arranged with a nearly perfect twofold symmetry (Fig. 8) (*36*). The BC-b rings of P are nearly parallel to the symmetry axis. The different degree of nonplanarity of the two BC-b–ring systems of P causes a deviation from symmetry. The BC_{MP} ring is considerably more deformed than that of BC_{LP}. This can cause an unequal charge distribution between the two components of P, which in turn can be part of the reason for unidirectional electron transfer (*37*).

Even though the tetrapyrrole rings of the BC-b's and BP-b's of the L and M branches can be rotated on top of each other by using a single transformation with the reasonably low rms deviation of 0.38 Å between the positions of equivalent atoms, a closer inspection shows considerable differences between the local symmetry operations of P, accessory BC-b's, and BP-b's. Imperfect symmetry causes the interatomic distances and interplanar angles to be different in both branches. For example, the closest distance of atoms involved in double bonds in P and BP_L is shorter by 0.7 Å than the corresponding distance between P and BP_M. These structural differences lead to different electron transfer properties in both branches. This may be another contribution to the unidirectional charge separation in the reaction center.

Protein-pigment interactions. A close view of the structures that are directly involved in the first step of the light-driven electron transfer reaction are shown in Fig. 9: P, the accessory BC-b BC_{LA}, and the first electron acceptor, BP_L. BC_{LA} is in van der Waals contact to both P and BP_L. The closest approach between the tetrapyrrole rings of P and BP_L is 10 Å (atoms in double bonds). The phytyl chain of BC_{LP} follows a cleft formed by BC_{LA} and BP_L; it is in van der Waals contact to both tetrapyrrole rings.

This arrangement suggests that the electron should follow the path $P \rightarrow BC_{LA} \rightarrow BP_L$. However, attempts to observe bleaching of the absorption bands of BC_{LA} caused by transient reduction failed. Spectroscopic experiments done with ultrafast laser systems indicated direct reduction of BP_L from P* without intermediate steps (*27, 28, 38*). This result has initiated an intense debate on the mechanism of electron transfer from P to BP_L and on the role of BC_{LA} in this process. As indicated with the example of Tyr M208 in Fig. 9, it seems plausible that the protein is important, not only as a scaffold to keep pigments in place, but also in influencing functional properties.

Numerous protein-pigment interactions are apparent also for P itself (*39*) (Fig. 10). These interactions include bonds between Nε atoms of His L173 and M200 to the Mg^{2+} ions of BC_{LP} and BC_{MP}, respectively. Both acetyl groups of P are hydrogen bonded: BC_{LP} to His L168 and BC_{MP} to Tyr M195. A further hydrogen bond is found between the ring V keto carbonyl oxygen and Thr L248; there is no equivalent hydrogen bond for BC_{MP}. The P environment is rich in aromatic residues: five Phe's, three Tyr's, and three Trp's are in direct contact with the tetrapyrrole rings of P. Tyrosine L162 is located between P and the closest heme group (HE3) of the cytochrome, and may be important during reduction of P^+ by the cytochrome (*39*).

BP_L, the first electron acceptor, with its protein environment is shown in Fig. 11, (*39*). The BP-b's are held in their places by noncovalent interactions only. In the positions where His ligands of BC-b's would be expected, we find Leu M212 for BP_L (Fig. 11) and Met L184 for BP_M. BP_L forms two hydrogen bonds with the protein. The one between the ring V ester carbonyl group and Trp L100 has an equivalent in a hydrogen bond between BP_M and Trp M127. The other hydrogen bond, between the ring V keto carbonyl oxygen and Glu L104 occurs in the L branch, as in the M side this residue is Val M131. Glutamic acid L104 is conserved in all currently known sequences of reaction center L subunits from purple bacteria. Its position in the electron transfer pathway strongly suggests that it is protonated; otherwise, the negative charge of the ionized Glu side chain would make electron transfer to BP_L energetically highly unfavorable.

As for P, aromatic residues are found in the vicinity of the BP-b's; the BP_L region is richer in aromatic residues than that of BP_M. The side chain of Try M250 forms a bridge between BP_L and the next electron acceptor, Q_A. The M-branch residue equivalent to Trp M250 is Phe L216, which cannot perform a similar bridging function between BP_M and Q_B.

The environment of the quinones and the nonheme iron (*39*) is shown in Fig. 12. Instead of Q_B, the figure shows the herbicide terbutryn in the Q_B binding pocket. The nonheme iron appears in the center of the drawing, between the binding sites of Q_A and Q_B, very near the central local twofold symmetry axis. It is bound by five protein side chains, four His's (L190, L230, M217 and M264), and Glu M232, of which the carboxylate group acts as a bidentate ligand. The iron sits in a distorted octahedral environment with the axial ligands His L230 and His M264, and equatorial ligands His L190, His M217, and Glu M232. The His residues L190 and M217 also contribute significantly to the binding of Q_B and Q_A, respectively. The location of the iron and its binding to residues from subunits L and M immediately suggests that part of the role of iron is to increase the structural stability of the reaction center. It is surprising that its role in electron transfer between the quinones seems to be relatively minor (*40*).

The head group of Q_A is bound in a highly hydrophobic pocket; its carbonyl oxygen are hydrogen bonded to the peptide NH of Ala M258, and to the Nδ of the iron ligand His M217. As mentioned above, Trp M250 forms part of the binding pocket of Q_A; its indole ring is nearly parallel to the head group of Q_A at a distance of 3.1 Å. The isoprenoid side chain of Q_A is folded along the surface of the L-

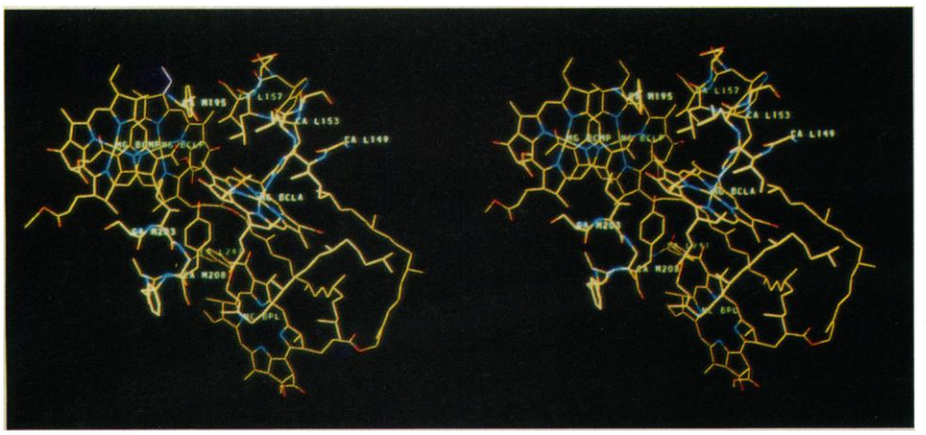

Fig. 9. Stereo view of P, BC_{LA}, BP_L, and selected residues in atom colors.

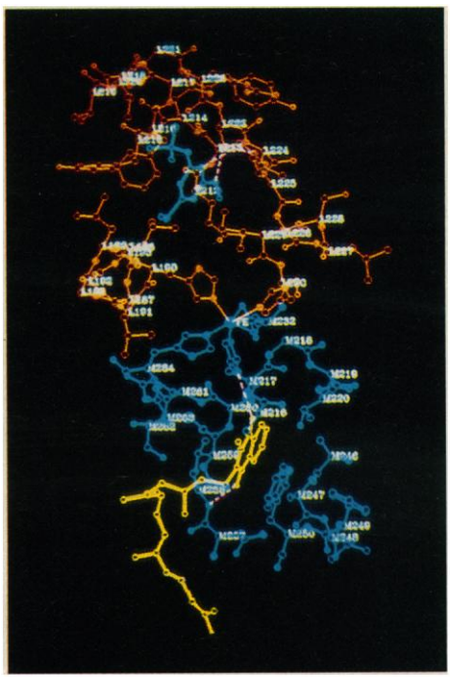

Fig. 12. Q_A, the nonheme iron, the herbicide terbutryn in the Q_B binding pocket, and the protein environment of these cofactors, colored as in Fig. 10 (*39*).

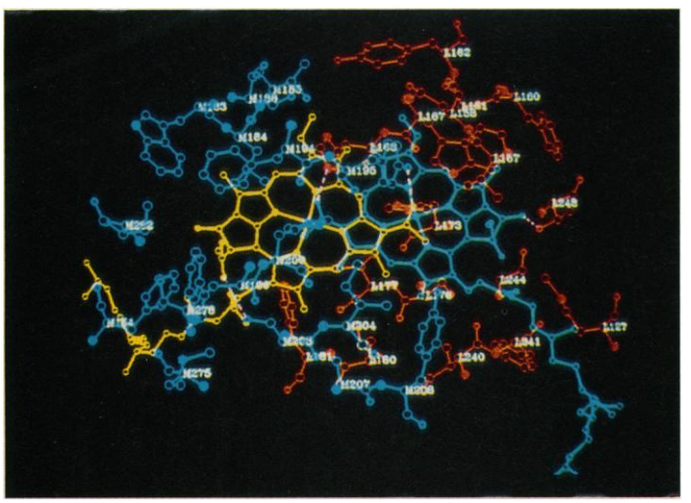

Fig. 10. P and its protein environment (*39*). Brown, residues from the L subunit; blue, residues from the M subunit and BC_{LP}; yellow, BC_{MP}. Hydrogen bonds are indicated in purple. The hydrogen bond between Ser M203 and BC_{MP} is no longer present in the refined model.

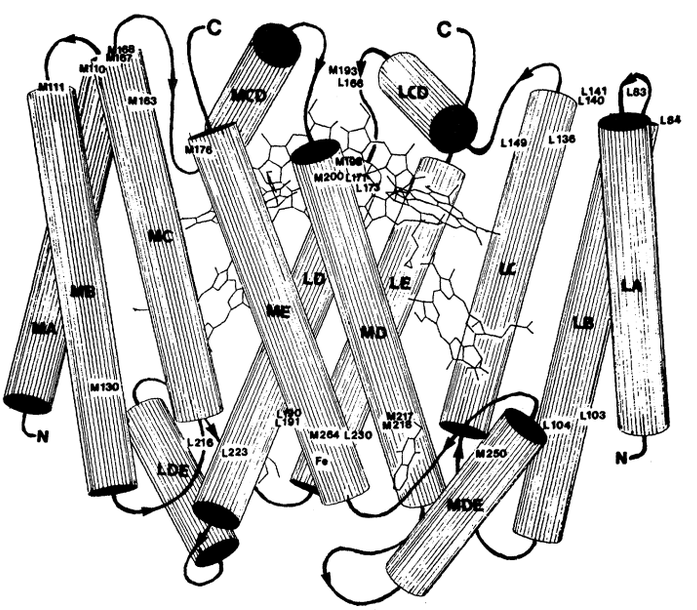

Fig. 13. Column model for the core of the reaction center from *Rps. viridis*. Only helices that are presumably conserved in photosystem II reaction centers are shown. The connections of the helices are only indicated schematically. The transmembrane helices of the L (M) subunit are labeled by LA-LE (MA-ME) and the major helices in the connections by LCD (MCD) and LDE (MDE). P's are at the interface of the L and M subunits between the D and E helices, and the BP's are near the L helices. The binding site for Q_A is between the LDE and LD helices. The location of the amino acids conserved between all L and M subunits and the D1 and D2 proteins, as well as those forming the quinone binding sites, is indicated by their sequence numbers (*42*).

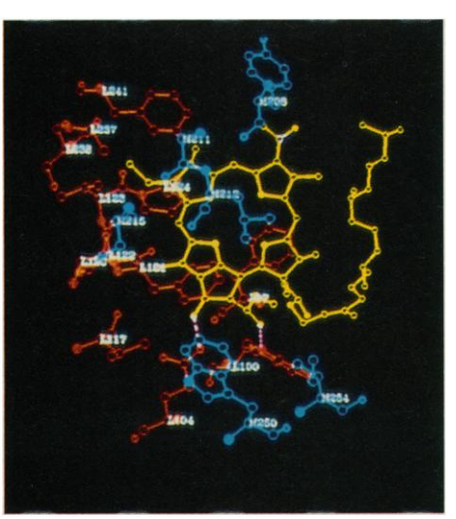

Fig. 11. BP_L (yellow) and its protein environment, colored as in Fig. 10.

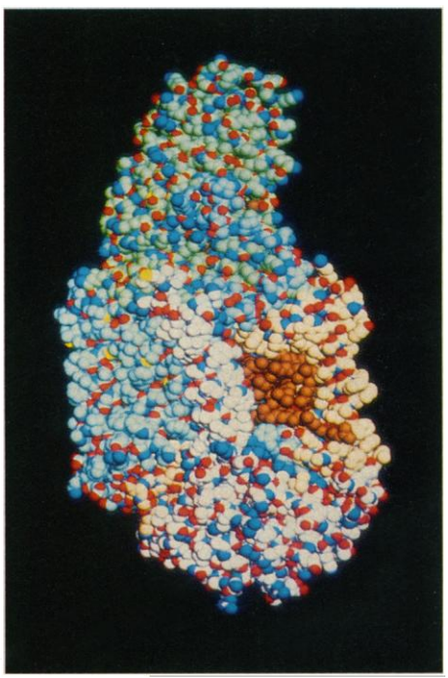

Fig. 14. Space-filling model of the photosynthetic reaction center from *Rps. viridis*. Carbon, white; nitrogens, blue; oxygens, red; and sulfurs, yellow. Atoms belonging to prosthetic groups are shown in brown.

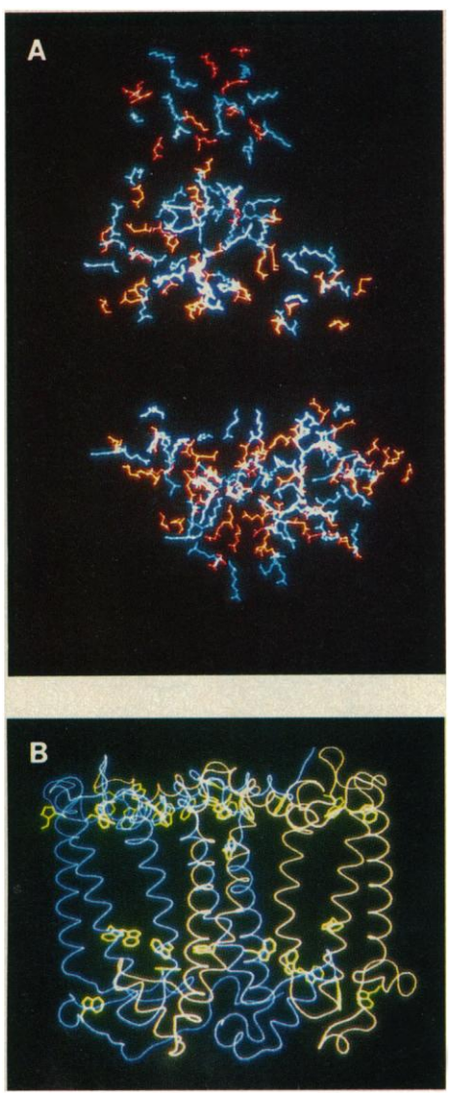

Fig. 15. (**A**) Distribution of the "charged" amino acids in the photosynthetic reaction center from *Rps. viridis*. The negatively charged amino acids (Asp and Glu) are shown in red, the positively charged amino acids (Arg and Lys) in blue. (**B**) Distribution of tryptophan residues (green) in the L (beige) and M subunits (blue).

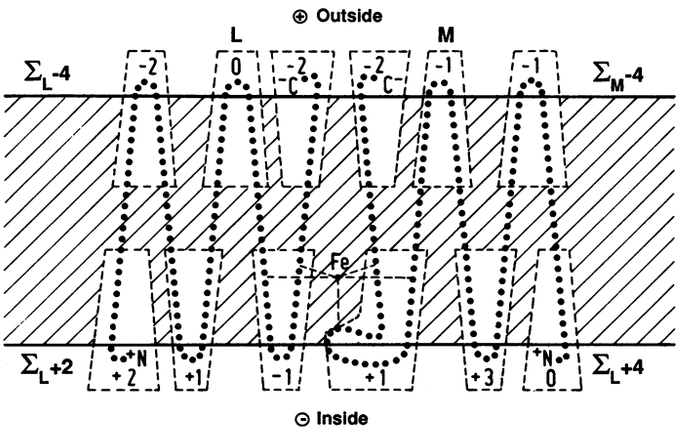

Fig. 16. Schematic drawing of the transmembrane helices, and the helix connection of the L and M subunits from *Rps. viridis* reaction center in the membrane, shows the net charges at the ends of the helices and the helix connections. The negatively charged interior of the cell is indicated by the minus sign at the bottom, the positively charged extracellular medium by the plus sign at the top (*67*).

M complex; the last three isoprenoid units are disordered in the crystal. The Q_A binding pocket is well shielded from the cytoplasm by the globular domain of the H-subunit.

Since the Q_B binding site in the reaction center crystals is only partially occupied, the Q_B model is less reliable than the other parts of the structural model discussed above. Nevertheless, the crystallographic data suggested a highly plausible arrangement of the Q_B head group in its pocket; the Q_B side chain remained undefined. It appears that Q_B, similar to Q_A, forms hydrogen bonds to the protein with its two carbonyl oxygens: one to the Nδ atom of the iron ligand His L190, and a bifurcated hydrogen bond to Oγ of Ser L223, and to NH of Gly L225. As Trp M250 for Q_A, Phe L216 forms a significant part of the Q_B binding pocket. Major differences between the binding sites of Q_A and Q_B are the more polar nature of the Q_B site and the presence of pathways through the protein, through which protons may enter the Q_B site. The bottom of the Q_B site is formed to a large part by the side chain of Glu L212. Protons can move from the cytoplasm along a path marked by charged or polar residues to Glu L212 and from there, by an as yet unknown mechanism, to the doubly reduced Q_B^{2-}.

The Relation to Photosystem II and Evolutionary Aspects

Conclusions on the structure of photosystem II reaction center. The most surprising result of the x-ray structure analysis was the discovery of the nearly symmetric arrangement of the reaction center core formed by the homologous L and M subunits together with the pigments. Primary electron donor as well as the ferrous nonheme iron atom are found at the interface between both subunits. Both subunits are needed to establish the reaction center.

During the x-ray structure analysis, the following results suggesting a close relation between the reaction centers from purple bacteria and photosystem II (*41, 42*) were or became available. (i) The photosystem II reaction center and the reaction center from purple bacteria both possess two pheophytin molecules (*43, 44*). Removal or the previous reduction of the quinones allows one electron to be trapped on one of the pheophytins (*45, 46*). (ii) Both reaction centers possess a magnetically coupled Q_A-Fe-Q_B complex. (iii) The L subunit of the purple reaction center and the D1 protein (which is the product of the *psbA* gene and also called Q_B protein, 32-kD

protein, or herbicide-binding protein) bind the herbicide azidoatrazine on photoaffinity labeling (*47, 48*). (iv) Weak but significant sequence homologies between the L and M subunits of the purple bacteria (*14, 49–51*), the D1 (*52*), and later on also D2 proteins (*53–56*) of photosystem II were discovered. The meaning of the results was obvious: the reaction center of photosystem II from plants and algae had to be formed by the D1 and D2 proteins with D1 corresponding to the L subunit and D2 corresponding to the M subunit. This proposal was at variance with the accepted view that the "CP47," a chlorophyll-binding protein with apparent molecular weight of 47,000, is the apoprotein of the photosystem II reaction center (*57*).

Several important differences exist between the reaction centers of photosystem II and the purple bacteria: the amino acids involved in the binding of the accessory BCs in the purple bacteria and the glutamic acid, which is a bidentate ligand to the ferrous nonheme iron, are not conserved. There is no hint for the existence of an analog to the H subunit in the photosystem II reaction center. The overall structure of the photosystem II reaction center core, however, must be very similar to the reaction center from purple bacteria formed by the L and M subunits. Helices that are presumably conserved between the reaction center cores of the purple bacteria and photosystem II, and the position of the amino acids conserved between the L and M subunits and the D1 and D2 proteins, are shown in Fig. 13. Identities of amino acids that are found specifically in the L subunits and D1 proteins, or specifically in the M subunits and D2 proteins, and involved in the quinone binding might be the result of convergent evolution (*13*). The re-reduction of the photooxidized primary electron donor occurs from the cytochrome subunit in the reaction center from *Rps. viridis*. In the position equivalent to the cytochrome subunit, we have to expect the water-soluble proteins that form part of the manganese-containing, oxygen-evolving complex in the photosystem II reaction center. Experimental proof for the existence of a similar reaction center core in photosystem II was the recent isolation of a complex consisting of the proteins D1, D2, and cytochrome b559 from spinach chloroplasts, which contained four to five chlorophylls and two pheophytins (*58*). This complex has been shown to be active in electron transport to the pheophytins. Evidence has been presented by two groups that a Tyr residue located on the D1 subunit in the third transmembrane helix is an intermediate electron carrier between the primary electron donor of photosystem II and the oxygen-evolving manganese cluster (*59, 61*). At present it is speculated if even the manganese cluster is bound to the D1 and D2 proteins. The work on the bacterial photosynthetic reaction center, has changed our entire view on the photosystem II reaction centers from plants and algae.

Evolutionary aspects. The sequence similarities discussed above suggest that the reaction centers from purple bacteria and photosystem II are evolutionary related. A common ancestor possessed an entirely symmetric reaction center with two parallel electron-transporting pigment branches across the membrane. In this view the symmetric reaction center was formed by two copies of the same protein subunit encoded by one gene. After a gene duplication and subsequent mutations, the formation of the asymmetric dimer and the use of only one pigment branch for electron transfer became possible. It is an open question if in evolution this gene duplication occurred only once, before the lineages leading to the purple bacteria and the photosystem II–containing organisms split, or twice, after the splitting into these two lineages. In the latter case the specific sequence similarities between L and D1, as well as those between M and D2, would be the result of convergent evolution, whereas the identities of the structurally important amino acids would date back to the original symmetric dimer. Sequence comparisons are in favor of the latter possibility (*62*): the sequence identity between the D1 and D2 proteins is much higher than those between the L and M subunits. This observation possibly indicates that the gene duplication giving rise to separate D1 and D2 proteins occurred later during evolution than the gene duplication leading to the L and M subunits. On the other hand, due to more and stronger interactions with neighboring proteins, the D1 and D2 proteins had less freedom to mutate than the L and M subunits. As a result, sequence comparisons might be misleading.

The evolutionary relations also indicate that there must be an advantage for reaction centers possessing only one active electron transport chain with two quinones acting in series. There might be rather trivial explanations for the use of only one branch, for example, an asymmetry in the protein environment can cause an asymmetry in the distribution of electrons in the excited state and subsequently lead to a preferred release of an electron only in one direction. This existing polarity might lead to a faster rate of the first electron transfer step, a minimization of competing reactions and thus a higher quantum yield for the electron transfer.

It is a clear advantage in the present day's reaction centers that the two quinones act in series, and only the released secondary quinone, Q_B, is a two-electron carrier. Consider the situation of the ancient symmetric reaction center: on the first excitation, the electron is transferred to the quinone at the end of one pigment branch. The resulting semiquinone is not stable and its electron is lost in seconds. Only if it receives a second electron can it be protonated and the energy stored in the form of the quinol. With two identical parallel electron transfer chains, the probability for the second electron to be funneled into the same chain to the same quinone as the first electron is only 50%. A possible electrostatic repulsion by the negatively charged semiquinone might even decrease this probability. In a frequent situation, the absorption of two photons leads to the formation of two semiquinones in the same reaction center, and energy is not stored in a stable way. The way out of this dilemma is to switch the two quinones in series and to allow protonation and release only to the final quinone, which is then Q_B in the electron transfer chain, as it is seen in the reaction centers of purple bacteria and photosystem II. A considerable increase in the efficiency of light-energy conversion, especially under low light conditions, must result.

Aspects of Membrane Protein Structure

The membrane anchor of the cytochrome subunit. The x-ray structure analysis established that the L and M subunits are firmly integrated into the membrane, both possessing five transmembrane helices, whereas the H subunit is anchored to the membrane by one transmembrane helix. The x-ray work showed no indication of any intramembranous part of the cytochrome subunit. Nevertheless, in the hands of the biochemists it behaved like a membrane protein and aggregated easily. A strange observation during the protein sequencing was that on Edman degradation of the isolated cytochrome subunit no NH_2-terminal amino acid could be identified after the first degradation, but a normal sequence could be obtained starting with the second amino acid from the NH_2-terminus. Mass spectrometry experiments showed that the NH_2-terminal amino acid is a Cys linked to a glycerol residue via a thioether bridge (*22*). Two fatty acids are then esterified to the two OH groups of the glycerol. The fatty acids are a statistical mixture of singly unsaturated C_{18} fatty acids and hydroxylated C_{18} fatty acids. These experiments firmly established that the cytochrome subunit also possesses a membrane anchor, but this is now of a lipid type and not of a peptide type. The membrane anchor is very similar to that of the bacterial lipoproteins (*63, 64*). The reaction center cytochrome subunit is the first

cytochrome molecule known to contain such a membrane anchor.

Protein-lipid contacts. From studying the percentage of the reaction center's "accessible surface area" that is covered by carbon atoms (Fig. 14), two important conclusions can be drawn. (i) The primary electron donor (P), is located in the hydrophobic nonpolar part of the membrane, whereas the nonheme Fe atom is already in that zone where the protein surface is polar and most likely interacts with the polar head groups of the lipids. (ii) The thickness of the hydrophobic zone perpendicular to the membrane is 30 to 31 Å only. This value is smaller than expected for a lipid bilayer composed of lipids with C_{18} fatty acids.

Distribution of amino acids. The distribution of the strongly basic amino acids Arg and Lys, and of the strongly acidic amino acids Glu and Asp, which at neutral *p*H possess electric charges at the ends of their side chains, is shown in Fig. 15A. A central zone, where none of these amino acids is found, has a thickness of about 25 Å and is thus slightly thinner than the hydrophobic surface zone. The slight discrepancy is due to two Arg residues and one Glu residue, which are apparently in a hydrophobic environment without counter charges. The role of the positive charges of the Arg side chains seem to be structural. They possibly cancel the partial negative charge at the COOH-terminal ends of the short helices in the connection of the long C and D transmembrane helices. These short helices partly intrude into the hydrophobic zone of the membrane, and a positive charge seems to be necessary for the change of the direction of the peptide chain. The Glu L104 seems to be protonated, thus neutral, and to form a hydrogen bond with one of the BPs (*39*).

Within the L and M subunits, the Glu and Asp and the Lys and Arg residues show an interesting asymmetric distribution with respect to cytoplasmic and periplasmic sides. If one calculates "net charges" of the peptide chains on the periplasmic side of the membrane and compares them with the net charges of the cytoplasmic side (assuming that all Glu residues, Asp residues, and the COOH-termini are negatively charged, whereas all the Arg and Lys residues and the NH_2-termini are positively charged), one finds that the cytoplasmic ends of the transmembrane helices and their respective connections are nearly always less negatively charged than their counter parts on the periplasmic side (Fig. 16). As a result, the cytoplasmic part of the M subunit carries four positive net charges and the periplasmic part carries four negative charges, the cytoplasmic part of the L subunit carries two positive charges and the periplasmic part carries four negative charges. The charge asymmetry becomes even more pronounced if one considers the existence of the firmly bound nonheme iron atom of the cytoplasmic side and the presumed protonation of Glu L104. Thus these membrane proteins are strong electric dipoles. This result can be correlated with the fact that the interior of bacteria is negatively charged, due to the action of electrogenic ion pumps. This means that the L and M subunits are oriented in the membrane in the energetically more favorable manner. Vice versa, the combination of the electric field across the membrane, established by the ion pumps, and the anisotropic distribution of negatively and positively charged amino acids in the protein may be one of the factors that determine the orientation of membrane proteins with respect to the inside and outside of the cell.

In the L and M subunits the remarkably uneven distribution of Trp (Fig. 15B) was quite unexpected. About two-thirds of the Trp are found at the ends of the transmembrane helices or in the helix connection on the periplasmic site. Only a few Trp residues are seen in the hydrophobic zone, where they are in contact with pigments. The residual Trp are located in the hydrophobic surface to polar transition zone or the polar part of the L and M subunits near the cytoplasmic hydrophobic surface. The indole rings of the Trp are oriented preferentially towards the hydrophobic zone of the membrane.

Crystal packing and detergent binding. As previously stated, the most promising strategy was to crystallize the reaction centers within the detergent micelles. According to this concept, the crystal lattice should be formed by polar interactions between polar surface domains of the reaction center. This expectation was confirmed by the results of the structural analysis. Mainly, the polar surfaces of the cytochrome subunit and the H subunit are involved in the crystal packing, and to a minor extent also the polar surface part of the M subunit.

As expected for detergents in a micelle, most of the detergent is crystallographically not ordered and cannot be seen in the electron density map with one exception: the single transmembrane helix of the H subunit, two transmembrane helices of the M subunit, and part of the pigments seem to form a pocket where one detergent molecule is bound. Its polar head group apparently undergoes specific interactions with the protein near the cytoplasmic end of the hydrophobic surface zone. Specific binding of this particular detergent molecule might explain why crystals of the photosynthetic reaction center from *Rps. viridis* could be grown only with *N*,*N*-dimethyldodecylamine *N*-oxide as detergent, but not when octylglucopyranoside or similar detergents were used.

In a collaboration with M. Roth and A. Bentley-Lewis, the detergent micelle was visualized by neutron crystallography and H_2O-D_2O contrast variation. A rather flat, monolayer-like ring of detergent molecules surrounding the hydrophobic surface zone of the reaction center became visible. Regions where the detergent micelles are in contact can also be seen. Therefore, attractive interactions between detergent micelles may also contribute to the stability of the protein's crystal lattice. In general, the strategy to crystallize membrane proteins within their detergent micelles (*4, 65*) now seems to be proven. However, the progress made in crystallizing membrane proteins other than bacterial photosynthetic reaction centers and bacterial porins has been unexpectedly slow: well-diffracting crystals of membrane proteins have only been obtained in these cases. The necessary fine tuning, with respect to the size of the detergent micelles and the size of the polar head group of the detergent, is still a formidable task that has to be solved empirically for each individual membrane protein.

REFERENCES AND NOTES

1. M. Happe and P. Overath, *Biochem. Biophys. Res. Commun.* **72** (no. 4), 1504 (1976).
2. D. Oesterhelt and W. Stoeckenius, *Nature* **233**, 149 (1971).
3. D. Oesterhelt, *Hoppe-Seyler's Z. Physiol. Chem.* **353**, 1554 (1972).
4. H. Michel, *Trends Biochem. Sci.* **8**, 56 (1983).
5. M. Zulauf, K. Weckstrom, J. B. Hayter, V. Degeorgio, M. Corti, *J. Phys. Chem.* **89**, 3411 (1985).
6. H. Michel, *EMBO J.* **1**, 1267 (1982).
7. R. K. Clayton and B. J. Clayton, *Biochim. Biophys. Acta* **501**, 478 (1978).
8. H. Michel, *J. Mol. Biol.* **158**, 567 (1982).
9. J. Deisenhofer, O. Epp, K. Miki, R. Huber, H. Michel, *ibid.* **180**, 385 (1984).
10. B.-C. Wang, *Methods Enzymol.* **115**, 90 (1985).
11. H. Michel, J. Deisenhofer, K. Miki, K. A. Weyer, F. Lottspeich, in *Structure and Function of Membrane Proteins*, E. Quagliariello and F. Palmieri, Eds. (Elsevier, Amsterdam, 1983), pp. 191–197.
12. J. Deisenhofer, O. Epp, K. Miki, R. Huber, H. Michel, *Nature* **318**, 618 (1985).
13. H. Michel, K. A. Weyer, H. Gruenberg, F. Lottspeich, *EMBO J.* **4**, 1667 (1985).
14. H. Michel *et al.*, *ibid.* **5**, 1149 (1986).
15. K. A. Weyer *et al.*, *ibid.* **6**, 2197 (1987).
16. A. Jack and M. Levitt, *Acta Crystallogr.* **A34**, 931 (1978).
17. J. Deisenhofer, S. J. Remington, W. Steigemann, *Methods Enzymol.* **115**, 303 (1985).
18. D. E. Tronrud, L. F. Ten Eyck, B. W. Matthews, *Acta Crystallogr.* **A43**, 489 (1987).
19. T. A. Jones, *J. Appl. Crystallogr.* **11**, 268 (1978).
20. P. V. Luzzati, *Acta Crystallogr.* **5**, 802 (1952).
21. J. Deisenhofer, O. Epp, I. Sinning, H. Michel, in preparation.
22. K. A. Weyer, W. Schaefer, F. Lottspeich, H. Michel, *Biochemistry* **26**, 2909 (1987).
23. P. Gast, T. J. Michalski, J. E. Hunt, J. R. Norris, *FEBS Lett.* **179**, 325 (1985).
24. W. W. Parson and B. Ke, in *Photosynthesis*, vol. 1, *Energy Conversion by Plants and*

Bacteria, Govindjee, Ed. (Academic Press, New York, 1982), pp. 331–384.
25. W. W. Parson, in *New Comprehensive Biochemistry: Photosynthesis*, J. Amesz, Ed. (Elsevier, New York, 1987), pp. 43–61.
26. C. Kirmaier and D. Holten, *Photosynth. Res.* **13**, 225 (1987).
27. J. Breton, J.-L. Martin, A. Migus, A. Antonetti, A. Orszag, *Proc. Natl. Acad. Sci. U.S.A.* **83**, 5121 (1986).
28. G. R. Fleming, J.-L. Martin, J. Breton, *Nature* **333**, 190 (1988).
29. W. Zinth, W. Kaiser, H. Michel, *Biochim. Biophys. Acta* **723**, 128 (1983).
30. W. Zinth *et al.*, *Chem. Phys. Lett.* **119**, 1 (1985).
31. E. W. Knapp, *et al.*, *Proc. Natl. Acad. Sci. U.S.A.* **19**, 8463 (1985).
32. R. J. Debus, G. Feher, M. Y. Okamura, *Biochemistry* **25**, 2276 (1986).
33. S. M. Dracheva, L. A. Drachev, A. A. Konstantinov *et al.*, *Eur. J. Biochem.* **171**, 253 (1988).
34. Ref. to P. Mitchell's theory.
35. J. R. Norris, R. A. Uphaus, H. L. Crepsi, J. J. Katz, *Proc. Natl. Acad. Sci. U.S.A.* **68**, 625 (1971).
36. J. Deisenhofer and H. Michel, in *The Photosynthetic Bacterial Reaction Center Structure and Dynamics*, J. Breton and A. Vermeglio, Eds. (Plenum, New York, 1988), pp. 1–3.
37. M. E. Michel-Beyerle *et al.*, *Biochim. Biophys. Acta* **932**, 52 (1988).
38. C. Kirmaier, D. Holten, W. W. Parson, *ibid.* **810**, 33 (1985).
39. H. Michel, O. Epp, J. Deisenhofer, *EMBO J.* **5**, 2445 (1986).
40. C. Kirmaier, D. Holten, R. J. Debus, G. Feher, M. Y. Okamura, *Proc. Natl. Acad. Sci. U.S.A.* **83**, 6407 (1986).
41. H. Michel and J. Deisenhofer, in *Encyclopedia of Plant Physiology, New Series: Photosynthesis III: Photosynthetic Membranes and Light Harvesting Systems*, L. A. Staehelin and C. J. Arntzen, Eds. (Springer, Berlin, 1986), pp. 371–381.
42. H. Michel and J. Deisenhofer, *Biochemistry* **27**, 1 (1988).
43. T. Omata, N. Murata, K. Satoh, *Biochim. Biophys. Acta* **765**, 403 (1984).
44. M. Y. Okamura, G. Feher, W. Nelson, in *Photosynthesis*, vol. 1, *Energy Conversion by Plants and Bacteria*, Govindjee, Ed. (Academic Press, New York, 1982), pp. 195–272.
45. D. M. Tiede, R. C. Prince, G. H. Reed, P. L. Dutton, *FEBS Lett.* **65** (no. 3), 301 (1976).
46. V. A. Shuvalov and V. V. Klimov, *Biochim. Biophys. Acta* **440**, 587 (1976).
47. C. de Vitry and B. A. Diner, *FEBS Lett.* **167** (no. 2), 327 (1984).
48. K. Pfister, K. E. Steinback, G. Gardner, C. J. Arntzen, *Proc. Natl. Acad. Sci. U.S.A.* **78**, 981 (1981).
49. J. C. Williams, L. A. Steiner, R. C. Ogden, M. I. Simon, G. Feher, *ibid.* **80**, 6505 (1983).
50. J. C. Williams, L. A. Steiner, G. Feher, M. I. Simon, *ibid.* **81**, 7303 (1984).
51. D. C. Youvan, E. J. Bylina, M. Alberti, H. Begusch, J. E. Hearst, *Cell* **37**, 949 (1984).
52. G. Zurawski, H. J. Bohnert, P. R. Whitfeld, W. Bottomley, *Proc. Natl. Acad. Sci. U.S.A.* **79**, 7699 (1982).
53. J. Alt, J. Morris, P. Westhoff, R. G. Herrmann, *Curr. Genet.* **8**, 597 (1984).
54. K. Holschuh, W. Bottomley, P. R. Whitfeld, *Nucleic Acids Res.* **12**, 8819 (1984).
55. O. F. Rasmussen, G. Bookjans, B. M. Stummann, K. W. Henningen, *Plant Mol. Biol.* **3**, 191 (1984).
56. J.-D. Rochaix, M. Dron, M. Rahire, P. Malnoe, *ibid.*, p. 363.
57. H. Y. Nakatani, B. Ke, E. Dolan, C. J. Arntzen, *Biochim. Biophys. Acta* **765**, 347 (1984).
58. O. Nanba and K. Satoh, *Proc. Natl. Acad. Sci. U.S.A.* **84**, 109 (1987).
59. R. J. Debus, B. A. Barry, G. T. Babcock, L. McIntosh, *ibid.* **85**, 427 (1988).
60. W. F. J. Vermaas, A. W. Rutherford, Ö. Hansson, *ibid.*, p. 8477.
61. C. W. Hoganson and G. T. Babcock, *Biochemistry* **27**, 5848 (1988).
62. J. C. Williams, L. A. Steiner, G. Feher, *Proteins Struct. Funct. Genet.* **1**, 312 (1986).
63. A. P. Pugsley, C. Chapon, M. Schwartz, *J. Biol. Chem.* **256**, 2194 (1986).
64. F. Yu, S. Inouye, M. Inouye, *ibid.* **261**, 2284 (1986).
65. R. M. Garavito, Z. Markovic-Housley, J. A. Jenkins, *J. Cryst. Growth* **76**, 701 (1986).
66. I. Sining and H. Michel, unpublished results.
67. H. Michel and J. Deisenhofer, *Chem. Scr.* **27B**, 173 (1987).
68. We wish to express our sincere gratitude to persons and organizations who helped to make our work possible and successful: Our colleagues Otto Epp, Heidi Gruenberg, Friedrich Lottspeich, Kunio Miki, Wolfram Schaefer, Irmgard Sinning, Karl-Alois Weyer, and Wolfgang Zinth made important direct contributions. Dieter Oesterhelt and Robert Huber, their departments, and the whole Max-Planck-Institut fuer Biochemie provided facilities and a stimulating and supportive atmosphere. Dieter Oesterhelt's backing up, especially during the initial, frustrating phases, and the stable environment in the Max-Planck-Gesellschaft allowed us to start a project of unknown duration and outcome. Smooth backbone representations of polypeptide chains were produced following an idea by R. J. Feldman with help from M. G. Clore. Financially, the project was supported by the Deutsche Forschungsgemeinschaft through Sonderforschungsbereich 143 (Teilprojekt A3 to H.M., Teilprojekt A6 to J.D. and H.M.) and the Max-Planck-Gesellschaft.

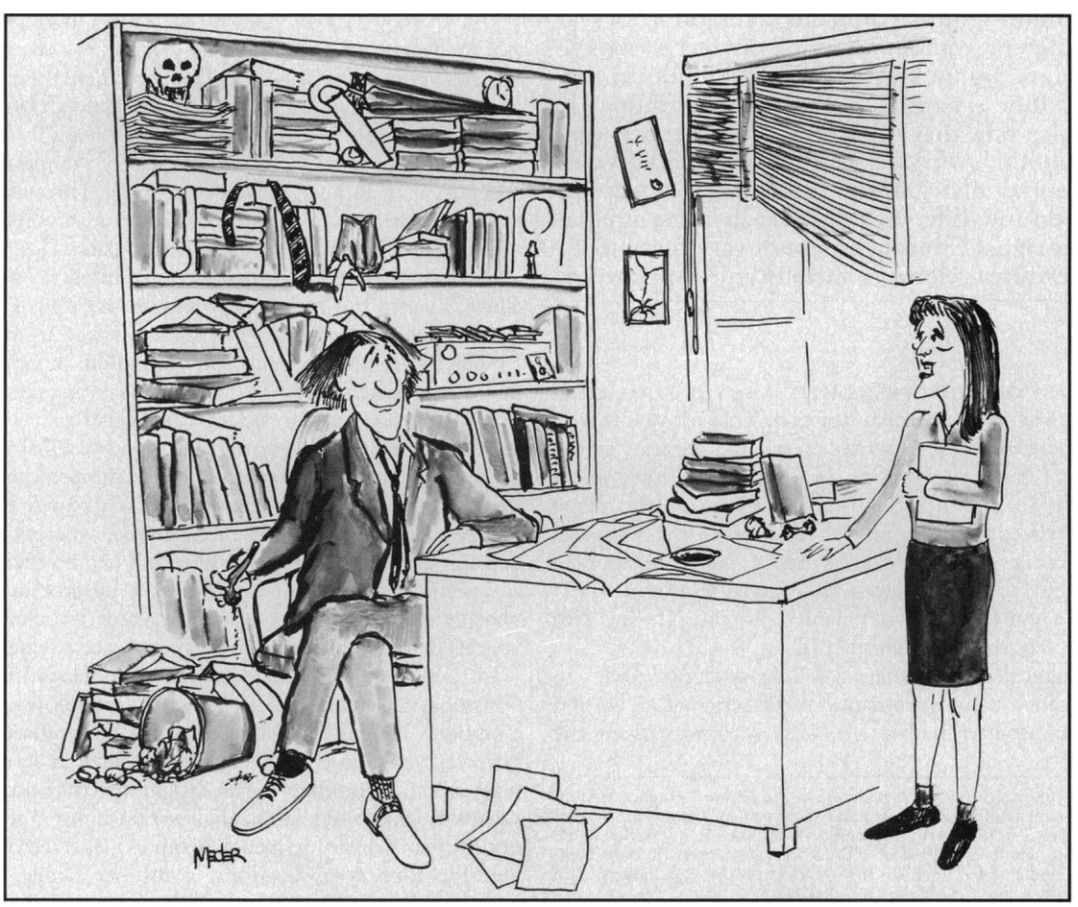

"What led you to the mathematics of chaos, Dr. Maynard?"